

UNUSUAL CONFORMATIONAL ASPECTS OF SOME NOVEL CHIRAL NON-RACEMIC PYRIDINYL-2-PHOSPHONATES^a

A.C. Dros,^b R.W.J. Zijlstra,^b P.Th. Van Duijnen,^b A. L. Spek,^c H. Kooijman^c and R.M. Kellogg^{b*}

^bDepartment of Organic and Molecular Inorganic Chemistry, University of Groningen, Nijenborgh 4, Groningen 9747 AG, The Netherlands

^cBijvoet Center for Biomolecular Research, Department of Crystal and Structural Chemistry, Utrecht University, Padualaan 8, 3584 CH Utrecht, The Netherlands

Received 15 January 1998; revised 24 April 1998; accepted 30 April 1998

Abstract:

Reaction of pyridinyl-2-phosphonyl dichloride (6) with 1-phenyl-2,2-dimethylpropane-1,3-diol (9) leads to the two epimeric 2-oxo-2-(2-pyridinyl)-4-phenyl-5,5-dimethyl-1,3,2-dioxaphosphorinanes (10a,b). These can be separated and the stereochemistry assigned on the basis of ³¹P NMR spectroscopy. For 10a the pyridinyl substituent is arranged axially at phosphorus. Arguments derived from 2D NMR experiments indicated that the nitrogen of pyridine is locked in a conformation whereby the pyridinyl nitrogen points over the six-membered ring; in other words it is locked between the two ring oxygen substituents. This conclusion is substantiated by an X-ray crystal determination. Oxidation of 10a with hydrogen peroxide leads to the N-oxide (12). The crystal structure of 12 reveals that despite serious steric overcrowding the N-O bond is also oriented over the six-membered ring. Methylation of 10a with methyl trifluoromethanesulfonate affords the N-methyl pyridinium salt (13). NMR experiments indicate that in this case the methylated nitrogen has turned "outside" of the six-membered ring. The borane adduct of 10a appears on the basis of NMR data to have a conformation wherein the complexed borane is located just outside of the six-membered ring. Although crystal structures have not been obtained the pyridinyl-2-thiophosphonates (15a,b) obtained from treatment of 10a and 10b with [(4-MeOC₆H₄)₂PS]₂ appear to have the same conformational properties as 10a and 10b. Restricted Hartree-Fock geometry optimizations have been carried out to aid in clarifying this unexpected conformational behaviour. These calculational results are in excellent accord with the experimental observations, and provide insight into the reasons for the conformational behaviour. © 1998 Elsevier Science Ltd. All rights reserved.

*Dedicated to Prof. Hans Wynberg on the occasion of his 75th birthday

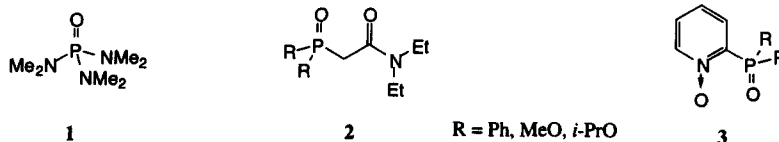
^bDepartment of Organic and Molecular Inorganic Chemistry

^cDepartment of Crystal and Structural Chemistry

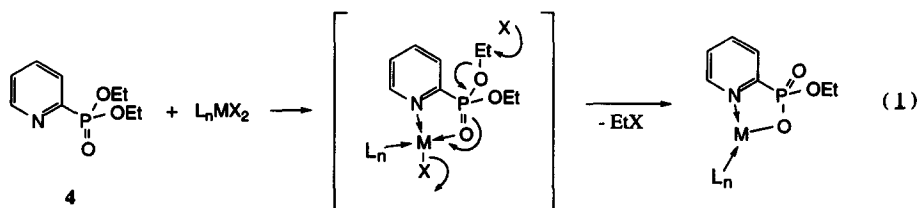
Introduction

Although phosphines have a well deserved reputation as *the* ligands for transition metals, more highly oxidized phosphorus compounds as simple in structure as trialkyl phosphine oxides and hexamethylphosphoric triamide (HMPA, **1**) show, for example, a high affinity for lanthanides and actinides, and are used to extract heavy metal ions from aqueous solutions.^{1,2} (Carbamoylmethyl)-phosphonates,³ (carbamoylmethyl)phosphine oxides⁴ (**2**), and pyridine N-oxides with phosphoryl groups in ortho-positions⁵ (**3**), all of which can function in a bidentate fashion, are effective ligators of various transition metal ions.

Various ligands based on phosphoryl groups have been described. In some cases one or more oxygen atoms may be replaced by the chalcogenides S, Se or Te, which serve as donor atoms toward transition metals.¹



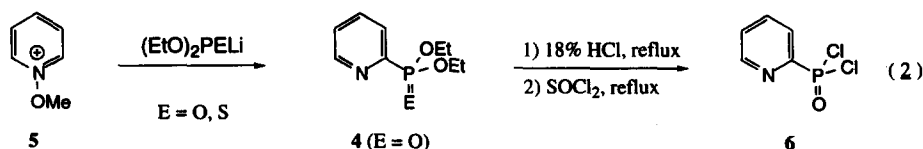
For instance, diphenyl-2-pyridinyl phosphine oxide complexes a variety of metals, ranging from iron⁶ to platinum.⁷ First row transition metals react with O,O-dialkyl pyridinyl-2-phosphonates in an Arbuzov-like manner, resulting in the extrusion of alkyl halide and formation of a mono-anionic O-alkyl phosphonate ligand (eq 1).^{8a}



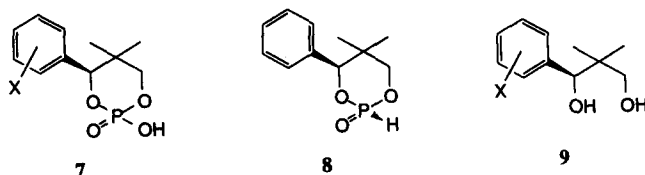
Copper (II) nitrates, perchlorates and tetrafluoroborates as well as ruthenium (III) and rhodium (III) chlorides, however, give isolable adducts with O,O-dialkyl-pyridinyl-2-phosphonates,^{8b,c,d} Bond lengths obtained from X-ray diffraction studies are consistent with metal-phosphoryloxygen bonds having multiple bond character, and M-O-P angles on various complexes vary from 113° to 180°. In contrast, M-E-P bonds (E=S, Se, Te) are single with angles varying from 96° to 120°.¹

Synthesis and Conformational Behaviour

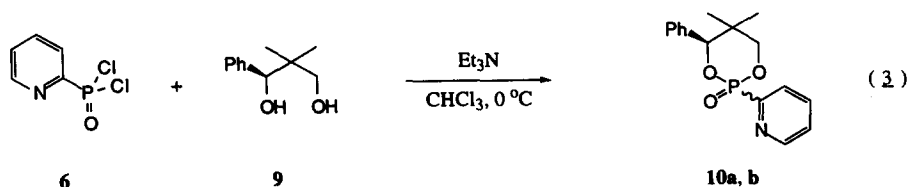
We became interested in applications of *chiral non-racemic* phosphoryl-containing ligands. As starting point the dichloride (**6**) was chosen, which is prepared by nucleophilic addition (eq 2) to the readily obtainable pyridinium salt (**5**).^{9,10,11} Subsequent hydrolysis and conversion to **6** are straightforward.^{9,12} The phosphonates (**4**) and the corresponding thiophosphonates have been studied as pesticides and insecticides, respectively.



Racemic chiral diols (**9**) are readily available and can be converted to the cyclic phosphoric acids (**7**) without problem. These cyclic phosphoric acids (**7** ($X=H$, 2-Cl, 2-OMe, etc) in chiral non-racemic form are superior resolving agents for a variety of amines and amino alcohols;¹³ the racemic phosphoric acids themselves are resolved with chiral non-racemic amino alcohols or amino acids. The enantiomerically pure phosphoric acids (**7**) provide the desired chiral non-racemic diols (**9**) on hydrolysis or reduction. Compounds **9** have been used, for example, as precursors for oxetanes and acetals.^{14,15} The hydrogen phosphonate (**8**) has been successfully applied as a derivatizing agent for the determination of enantiomeric excesses of alcohols, amines and amino acids using ³¹P NMR spectroscopy.¹⁶



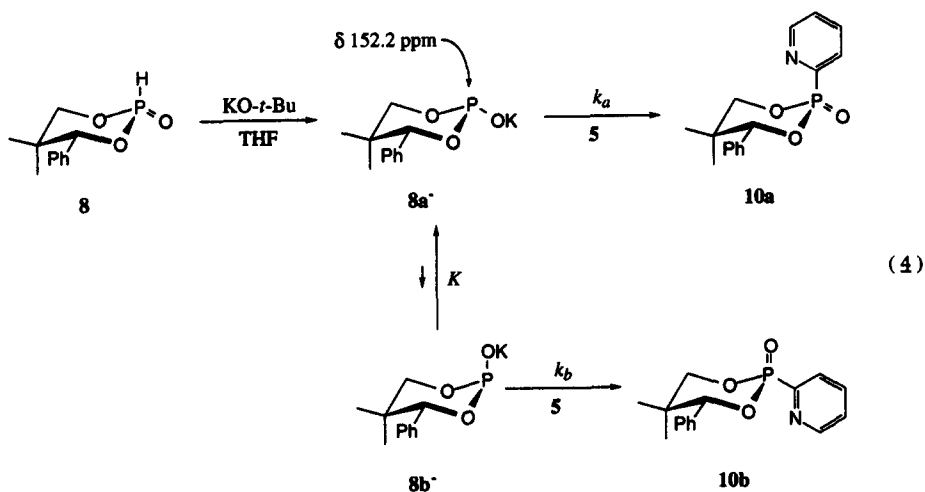
Reaction of **6** (eq 3) with enantiomerically pure 1-phenyl-2,2-dimethylpropane-1,3-diol **9** ($X=H$) leads to a mixture of two epimeric 2-oxo-2-(2-pyridinyl)-4-phenyl-5,5-dimethyl-1,3,2-dioxaphosphorinanes **10a,b**.



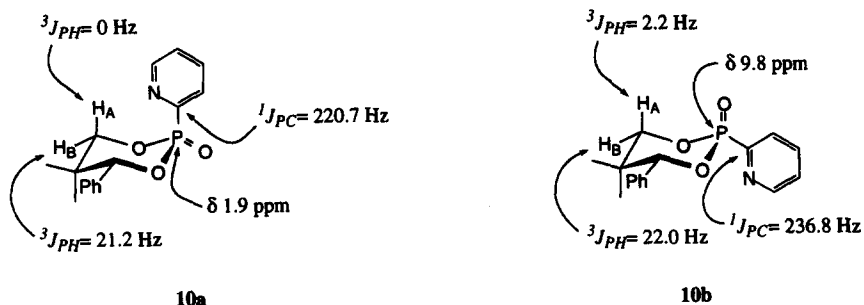
The epimers were separated by column chromatography and after crystallization **10a** and **10b** were obtained as white crystalline solids in 37% and 24% yields, respectively.

An alternative route allows better control over the distribution of epimers. Addition of the phosphonate salt (**8**), prepared from reaction of **9** with H_3PO_3 and dicyclohexylcarbodiimide,¹⁷ followed by treatment with Me_3COK , to **5** provides **10a** and **10b** in a 6:1 ratio. Owing to the easier purification the route of eq 4 is the preferred one to pure **10a**.

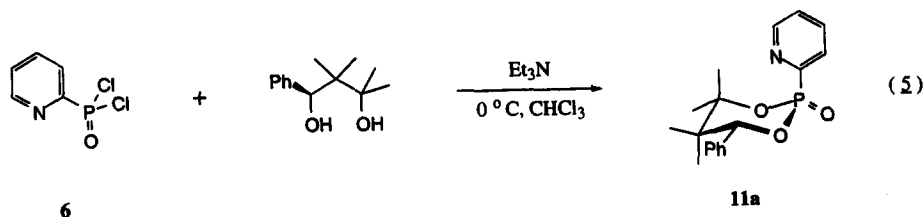
Alkali metal derivatives of dialkyl phosphonates like **8** are in fact dialkyl phosphite anions; the infrared spectra lack the P=O absorption band but have a strong band around 1050 cm^{-1} characteristic for $\text{R}_2\text{P-O}^-$ groups.¹⁸ The ^{31}P NMR resonances for these salts are observed in the phosphite range of the spectrum, consistent with the dialkyl phosphite anion formulation.¹⁹ Phosphite anions react as P-nucleophiles and equilibration of the anions is relatively slow. The kinetically formed anions can be trapped by adding base to a mixture of phosphonate and electrophile.¹⁹ In the ^{31}P NMR spectrum of the K^+ salt of **8** a single resonance at $\delta\ 152.2\text{ ppm}$ is observed; this is attributed to **8a**⁻. It seems reasonable that this anion reacts with **5** to give **10a** exclusively. If so, **10b** will be formed from reaction of **8b**⁻ with **5** (eq 4). The equilibrium constant K between **8a**⁻ and **8b**⁻ must be at least 99 (^{31}P NMR detection levels). Since the product ratio is equal to $(k_a/k_b)K$,²⁰ k_b must be at least 17 times greater than k_a in order to provide the observed product ratio. This is an example of the operation of the Curtin-Hammett principle.



The stereochemistry at the phosphorus center in **10a,b** should be assignable from the NMR spectra. For determination of the relative disposition of substituents three parameters are important; namely the ^{31}P chemical shift, the $^1J_{\text{PC}}$ coupling constant and the sum of the $^3J_{\text{PH}}$ coupling constants of the axial and equatorial hydrogen atoms at the 4- and 6-positions on the dioxaphosphorinane ring to the phosphorus atom. Generally, for the epimer having the phosphoryl oxygen atom in the axial position, ^{31}P chemical shifts are found at lower field and coupling constants are larger.^{21,22} For **10a,b** the values shown were found and the stereochemistry at phosphorus assigned accordingly (the absolute configuration of the carbon center is, of course, known via the synthetic route).



One observation was puzzling, however. In the high resolution NOESY spectrum of **10a** in C_6D_6 , despite repeated attempts using different mixing times, no NOE interactions between pyridinyl hydrogen atoms and axial hydrogen atoms of the dioxaphosphorinane ring could be detected. All other expected contacts were observed. The downfield shifts of the axial hydrogen atoms for **10a** (C_6D_6) of 6.03 and 4.93 ppm seem reasonable for the expected shielding of the aromatic ring; in **10b** these shifts are 5.43 and 4.35 ppm. One is drawn to the conclusion that if these stereochemical assignments are correct, the pyridinyl ring in **10a** must be locked in a conformation whereby the nitrogen atom points *towards* the axial hydrogens. Some of the shielding effect could arise from this, an idea which is supported by the observation that the downfield shift for the benzylic hydrogen atom increases upon introduction of two methyl groups (compound **11a**) at the 6-position of the dioxaphosphorinane ring (eq 5),⁷



forcing the pyridinyl moiety towards the benzylic position (δ ($CDCl_3$): 6.16 ppm for **11a** vs. δ 5.90 ppm for **10a**).

A crystal structure was determined to check this conclusion. Compound **10a** crystallizes from toluene/pentane in the orthorhombic space group $P2_12_12_1$ with two molecules in the asymmetric unit, which have two slightly different conformations, one of which is depicted in Fig. 1. Selected bond lengths and bond angles are given in Table 1 together with values obtained from restricted Hartree-Fock calculation (see next section for tables of structural and calculational results).

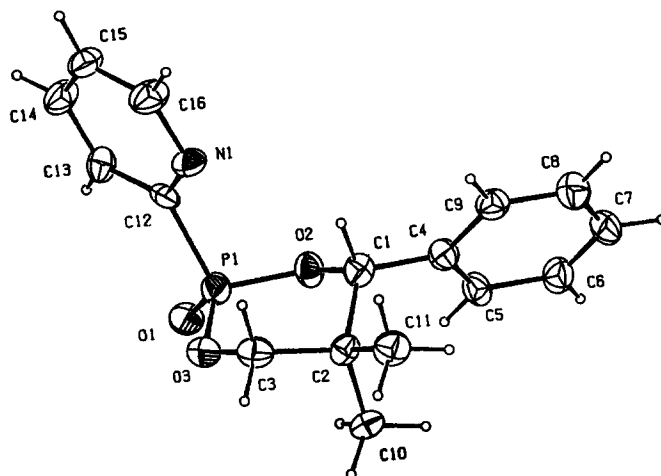
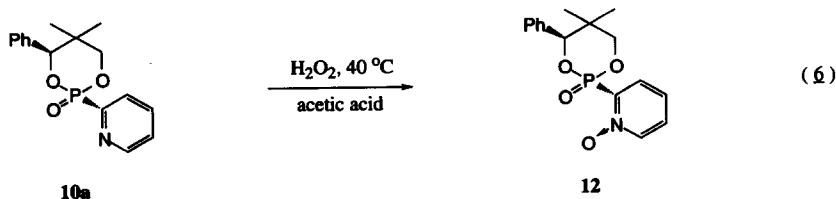


Fig. 1 Molecular structure of **10a** with numbering scheme.

The crystal structure is entirely consistent with the conclusions drawn from NMR experiments especially with regard to the orientation of the pyridyl ring. The 1,3,2-dioxaphosphorinane ring displays the typical chair conformation generally observed, although the ring is somewhat flattened at the phosphorus end; dihedral angles P-O2-C1-C2 and P-O3-C3-C2 are $+50.6(6)^\circ$ and $-49.1(6)^\circ$, respectively. In the second molecule of the asymmetric unit the dihedral angles have values of $+46.4(6)^\circ$ and $-50.0(6)^\circ$, respectively. These angles are slightly smaller than those in an “unstrained” phenyl phosphonate ($+/-53.5(2)^\circ$ and $+/-55.8(2)^\circ$).^{23b} Refinement of a disorder model that allowed the pyridinyl ring to be placed in a conformation with the N atom syn to the P=O bond resulted in an occupation factor for this alternative conformation of only 0.02(3). Further refinements were therefore carried out using a single conformation model.

Mutual repulsion of the oxygen and nitrogen lone pairs provides a tentative explanation of the pronounced conformational preference in **10a**; this point has been checked by calculations (*vide infra*). In solid state molecular structures of 2-phenyl-1,3,2-dioxaphosphorinanes the axial phenyl groups at phosphorus are oriented perpendicularly with respect to the phosphorus-oxygen double bonds.^{23a}

What does it take to change the “inward” conformation of **10a**? We noted the description of an unexpected *in situ* oxidation of the nitrogen atom of an aminophosphine oxide ligand on treatment with molybdic acid in aqueous H_2O_2 ; the N-oxide coordinates to the molybdenum atom.²⁴ This reaction was attempted with **10a** but neither oxidation nor coordination was observed. The N-oxide (**12**) of **10a** can be prepared, however, on use of H_2O_2 in acetic acid at $40^\circ C$ for two days (eq 6).



However, again for **12** no NOE effects between the pyridinyl hydrogens and the axial hydrogens were observed. The chemical shift behaviour in the ^1H NMR spectra was analogous to that of **10a**. In C_6D_6 (in which the signals are well separated) the axial hydrogens are shifted downfield to 6.46 and 5.38 ppm for **12** compared to 6.03 and 4.93 for **10a**. The implication is obvious; despite the distortion in the six-membered ring that must occur as indicated from molecular models, the oxygen of **12** must be directed back towards the ring.

This conclusion was confirmed by the crystal structure. The compound crystallizes in the orthorhombic space group $\text{P}2_12_12_1$ with one molecule in the asymmetric unit cell. The molecular structure of **12** indeed shows the expected “inward” orientation of the pyridine N-oxide ring (Fig. 2).

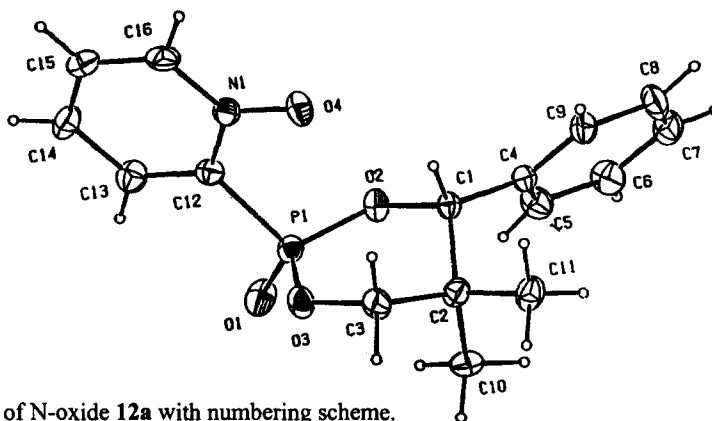
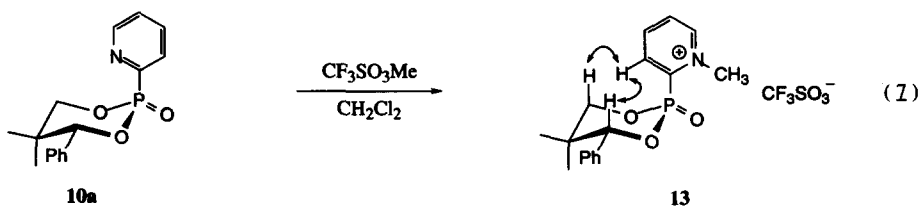


Fig.2 Molecular structure of N-oxide **12a** with numbering scheme.

In order to accommodate the oxygen atom, the flattened chair conformation found in **10a** is distorted to an envelope-like conformer, with atoms C1, O2, P1, O3 and C3 virtually coplanar (the maximum deviation from the least-square plane is 0.047(3) Å. Dihedral angles P-O2-C1-C2 and P-O3-C3-C2 are 39.0 (4)° and -31.8 (5)°, respectively. Selected bond lengths and angles as well as details on data collection and refinement are given in Table 1 (see next section).

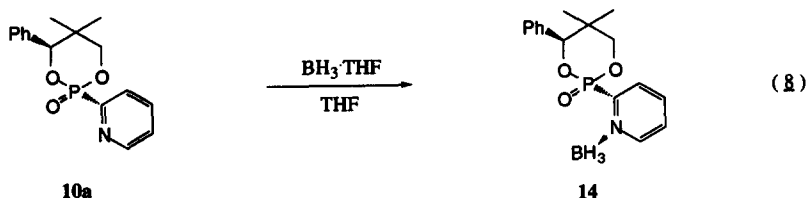
Unfortunately treatment of **10b** with H_2O_2 under conditions similar to those used for **10a** does not lead to any conversion and under more forcing conditions decomposition occurs.

If lone pair interactions are the cause of this conformational behaviour, protonation of **10a** should remove this effect. Unfortunately excess trifluoroacetic acid was incapable of protonating **10a** apparently because of the extremely low basicity of the nitrogen. Methylation was next tried and the N-methylated pyridinyl-2-phosphonate **13** was obtained on reaction of **10a** with excess methyl trifluoromethanesulfonate (eq 7).



The reaction with “magic methyl” is, however, very slow and takes several days to go to completion. The coupling patterns in the ^1H NMR spectrum of **13** are typical for a chair conformer; axial hydrogens show no $^3J_{\text{PH}}$, whereas the equatorial hydrogen atom shows a large $^3J_{\text{PH}}$ of 24.1 Hz. The trace (δ 8.28 ppm) of the NOESY spectrum of **13** shows interactions between the hydrogen atom at the 3-position on the pyridinyl fragment and both axial hydrogen atoms on the dioxaphosphorinane; the N-methyl hydrogens lack any NOE interactions with the latter; the arrows (eq 7) indicate the diagnostic NOE interactions. The conclusion is clear; the N-Me unit in **13** has (finally) turned “outward”.

One might well expect similar results with borane. The observed behaviour was more complicated, however. On treatment of **10a** with $\text{BH}_3 \cdot \text{THF}$ a white solid, tentatively assigned structure (**14**), precipitated (eq 8).



This can be stored for some time without decomposition. The NOESY spectrum (not illustrated) shows interactions between borane hydrogen atoms and the benzylic hydrogen of the dioxaphosphorinane unit. Interaction of the other axial hydrogen at C-6 with the borane protons or with the pyridinyl proton at the 3-position of the pyridine ring is not observed. These observations are consistent with rotation of the pyridine fragment around the P-C bond, placing the complexed borane outside the dioxaphosphorinane ring at the side of the phenyl group as illustrated in Fig. 3.

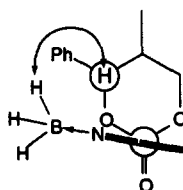
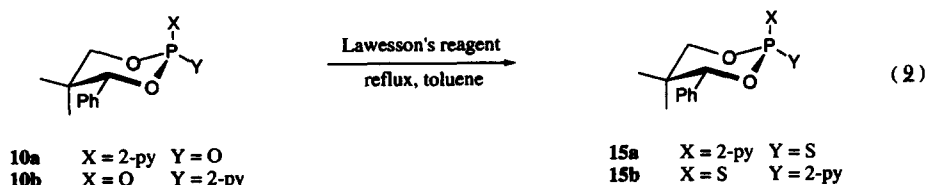


Fig. 3 Proposal binding mode of borane complex **14** based on NOESY spectra (top view).

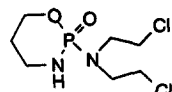
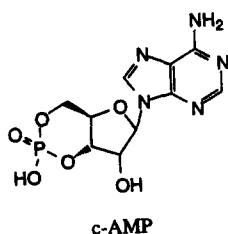
The synthesis and conformations of the corresponding pyridinyl-2-thiophosphonates were briefly examined. Treatment of **10a** and **10b** with Lawesson's reagent $[(4\text{-MeOC}_6\text{H}_4)_2\text{PS}]_2$ in boiling toluene (eq 9)



led to **15a** and **15b**, respectively. The reactions appeared to proceed stereospecifically although traces of the other stereoisomer could have been lost during work-up procedures. The ^1H NMR spectra of **14a** and **14b** closely resemble those of **10a,b**, respectively, indicating the same conformations of the 1,3,2-dioxaphosphorinane rings and identical configurations about the phosphorus atom. The ^{31}P NMR chemical shifts for **15a** and **15b** are 70.6 ppm and 79.9 ppm, respectively, also consistent with retention of configuration about phosphorus during reaction. Crystallographic structure determinations have not been carried out.

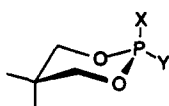
Computational Results

To understand better the reasons for this unusual conformational behaviour some calculational work has been done. Conformations of phosphorinanes, 1,3,2-diheterophosphorinanes in particular, have been widely studied.²⁵ Examples of 1,3,2-dioxaphosphorinanes and 1,3,2-oxazaphosphorinanes are found in physiologically active molecules such as the intracellular second messenger, cyclic adenosine monophosphate (c-AMP), and clinical antitumor agent, cyclophosphamide, respectively.^{26,27}

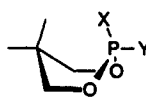


cyclophosphamide

In principle the three common conformations - chair, boat and twist boat - could be observed for these ring systems, all somewhat flattened at the phosphorus end owing to the relatively long P-O bonds. We have been able to rationalize all conformational behaviour in terms of chair conformations as described below.



chair

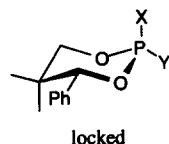


boat



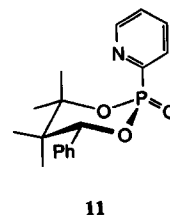
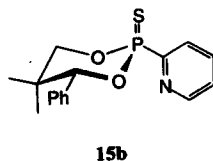
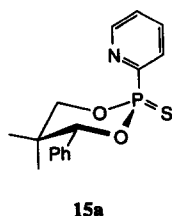
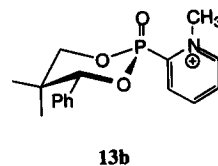
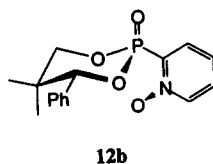
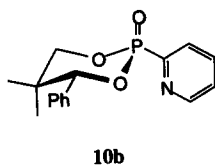
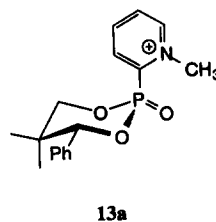
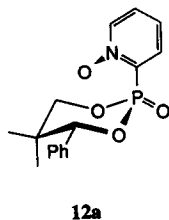
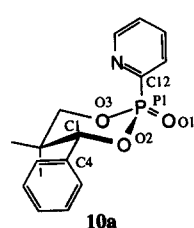
twist-boat

Chair conformations of 5,5-dimethyl-1,3,2-dioxaphosphorinane will be mobile (eq 10), but we may assume that addition of a phenyl group at the 4-position together with the 5,5-dimethyl groups (present work) will lead to an anancomeric molecule in which the substituents effectively lock the molecule in a single conformation.^{28,29,30}



Calculational work has been carried out on the set of compounds illustrated; some structures are repeated for clarity. X-ray data are available for **10a** and **12a** and NMR data for **10b**, **13a**, **14a,b** and **11**, which is included for comparison purposes. It has not been possible to synthesize **12b** (nitrogen apparently too hindered) or **13b**.

Restricted Hartree-Fock geometry optimizations of the compounds depicted were performed at the 3-21G level for all atoms except phosphorus and sulfur, for which an additional set of six cartesian d-type polarization functions was included (6-31G*). Inclusion of these d-type functions is a requirement for the accurate reproduction of experimentally observed bond lengths around phosphorus. Geometry optimization at the 6-31G* level for all atoms would have resulted in unacceptable increase in cpu times.



The Hartree-Fock calculations of the compounds described, consisting of at least 39 (**10**, **14**) to 45 (**11**) atoms and having C1 symmetry, requires 207 to 260 basisfunctions.

Although the use of unbalanced basis sets in geometry optimizations can give rise to substantial basis set superposition error (BSSE) effects on geometry, the successful reproduction of solid state structures (*vide infra*) indicates that this is not a serious problem here.

The energies related to the minimized geometries for all structures under consideration were calculated at the RHF 6-31G* level for all atoms. Single point calculations of several non-optimized geometries were performed in order to estimate the energy barriers for rotation around the phosphorus-carbon bond. It should be noted that these single point geometries were generated from optimized global minima by only altering the dihedral angle of interest. Since non-optimized geometries were used, these energies reflect the upper limits of the rotational barriers.

Optimized geometries for **10a** and **12a** (Fig 4)

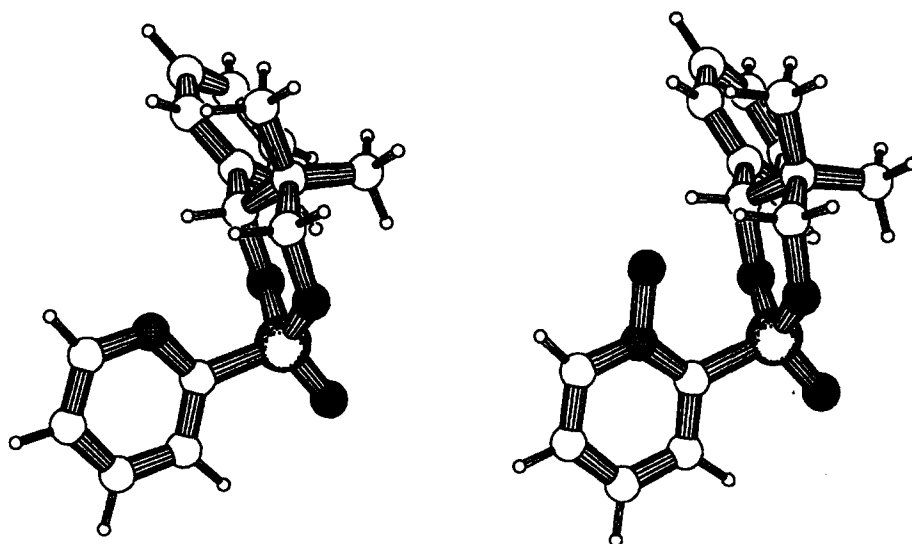


Fig 4. RHF 3-21G/6-13G* optimized geometries for **10a** (left) and **12a** (right)

show excellent correlations with the solid state structures. Data from solid state structures and RHF calculations are compared in Table 1.

Table 1. Geometrical data for 10a and 12a. RHF 3-21G/6-31G* vs. X-ray diffraction^a

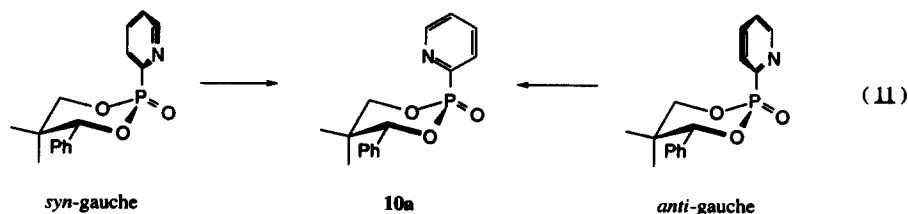
	10a	10a	10a	12a	12a	12a <i>syn gauche</i>	12a <i>anti gauche</i>
	RHF	mol 1 X-ray	mol 2 X-ray	RHF	X-ray	RHF	RHF
Energy (AU)^b	-1236.2078	-	-	-1310.9816	-	-1310.9654	-1310.9642
Bond lengths Å							
P1-O1	1.457	1.460(4)	1.461(5)	1.460	1.459(3)	1.453	1.453
P1-O2	1.589	1.575(4)	1.569(4)	1.574	1.568(3)	1.600	1.606
P1-O3	1.585	1.581(5)	1.569(5)	1.570	1.567(3)	1.580	1.576
P1-C12	1.800	1.789(6)	1.801(16)	1.817	1.805(5)	1.812	1.813
Bond angles (deg)							
O1-P1-O2	114.91	112.6(2)	112.8(2)	114.74	112.35(17)	113.05	116.20
O1-P1-O3	115.46	112.1(2)	112.4(3)	115.40	113.56(18)	116.67	113.53
O1-P1-C12	112.03	112.2(3)	111.0(3)	107.06	106.59(19)	115.67	116.06
O2-P1-O3	102.48	105.7(2)	105.9(2)	104.66	107.90(17)	101.71	101.89
O2-P1-C12	105.27	107.5(2)	106.2(3)	106.94	110.74(18)	98.51	108.01
O3-P1-C12	105.58	106.3(2)	108.2(3)	107.57	105.48(18)	108.91	98.94
Dihedral angles (deg)							
O1-P1-C12-N1	179.72	-178.7(4)	-170.2(5)	-179.74	-174.3(3)	-75.28	72.62
P1-O2-C1-C2	-51.15	50.6(6)	46.4(6)	-42.52	39.0(4)	-46.92	-52.70
P1-O3-C3-C2	48.81	-49.1(6)	-50.0(6)	39.21	-31.8(5)	50.77	40.85

^a estimated standard deviation for X-ray data in parentheses^b 1AU (atomic unit) = 627.51 Kcal mol⁻¹

Calculated bond lengths around the phosphorus atom are slightly longer (0.003–0.020 Å) than those obtained by X-ray; P=O double bonds are the same within standard deviation. Note that 10a consists of two similar but nonidentical molecules. Calculated angles (see Figs 1 and 2 for numbering schemes) O1-P1-O2 and O1-P1-O3 are larger by 2°, angles O2-P1-C12 and O3-P1-C12 are smaller by 2–3° and 1–4°, respectively. The deviation in the bond angles likely results from minor BSSE effects on the geometries. Except for the minor deviations in bond lengths and angles, the RHF optimized geometries of 10a and 12a are virtually identical to the solid state structures and justify the use of this mixed basis set. The dioxaphosphorinane ring in 10a is calculated to be an elongated chair and in 12a the ring is calculated to be flattened at the phosphorus end to accommodate the N-oxide; this is exactly in accord with the crystal structures.

What about the the orientation of the pyridine ring? We first examined 10a. The pyridine nitrogen is indeed calculated to be anti to the P=O double bond. This is apparently the result of repulsion of the lone pairs on O1 and nitrogen. But how large is this effect and how much movement is tolerated? We will try to sketch a picture of what is involved; the reader should realize, however, that the calculational work has not been exhaustive.

We guessed that conformational minima for 10a would include the *syn-gauche* and *anti-gauche* conformations shown in eq 11. Analysis of the calculational results indicates that this guess was correct for 12a but probably incorrect for 10a.



In these gauche conformations the nitrogen (or N-oxygen in the case of 12a) is positioned between endocyclic oxygen and phosphoryl oxygen lone pairs. However, optimization of 10a “manually” put in either gauche conformation does not lead to local minima; the structure relaxes towards the global minimum. Energy barriers associated with rotation about the phosphorus-carbon bond were estimated from the single point energies of the non-optimized conformations generated from the global minimum energy conformation of 10a. For this, dihedral angles O1-P-C12-N, O2-P-C12-N and O3-P-C12-N were set at 0° (eclipsed conformations between pyridine C=N and P-O bonds). The energy differences for these points are 15.1, 4.1 and 3.9 kcal/mol. For energy barriers of 15 kcal/mol bond rotation on the NMR time scale will be sufficiently slow that the conformation will appear to be frozen. Because local minima for the gauche conformations of 10a could not be obtained, the corresponding geometries for 12a, for which minima were found (*vide infra*), were taken (-75.25° and 72.62°). Calculated energies for syn-gauche 10a and anti-gauche 10a are 11.1 and 11.4 kcal/mol higher than the global minimum. The pyridinyl segment can swing (roughly a 120° swing in total) appreciably away from the global minimum and can even eclipse the oxygens O2 and O3 without a high energy price. Further deviation leads to rapid increase in energy. This behaviour would be fully consistent with the lack of observed NOE contacts.

As seen from Fig 5

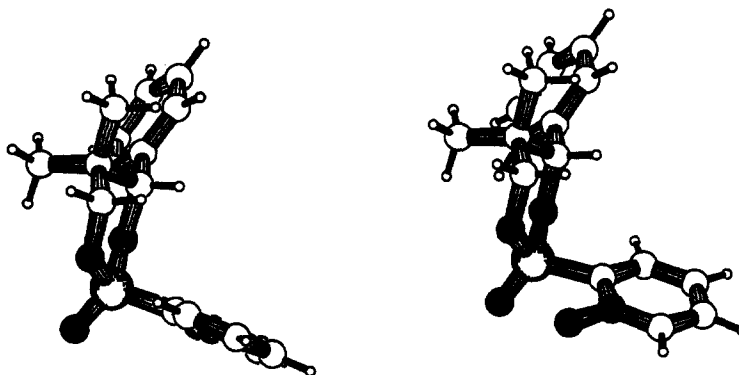


Fig 5. RHF 3-21G/6-31G* optimized syn-(left) and anti-gauche (right) geometries of 12a

gauche conformations are indeed local minima for N-oxide 12a. Single point calculations show these to be higher in energy than the global minimum conformation by 10.16 and 10.91 kcal/mol for the *syn*- and *anti*-conformations, respectively. Apparently the N-oxide cannot readily eclipse O2 and O3. The dihedral angles *theta*, defined by O1(O2)-P-C12-N, are -75.25° and 72.62°, respectively. From the angles O2-P1-C12 (98.5° and 108.0°) and O3-P1-C12 (108.91° and 98.94°) it can be seen that the pyridinyl fragment is tilted backwards to minimize repulsions. Single point energies of non-optimized geometries of 12a with *theta* set “manually” at 0° were calculated to estimate the rotational barrier (attempts to calculate the rotational barriers of 12a in the semi-empirical AM1 package resulted in gradual change of the ring conformation to a twist-boat). Values of 34, 18 and 17 kcal/mol, respectively, were obtained starting from the optimized geometry of the global minimum for 12a. In view of the energy differences between the gauche conformations and the local minimum (anti with respect to P-O1), chiefly the latter should be populated at room temperature.

As already mentioned, NOE interactions between the pyridinyl ring and other hydrogens are absent in **10b**. An “inward” conformation is expected. Crystallographic data are not available but the calculation data indicate that this is so. The structure is illustrated in Fig. 6.

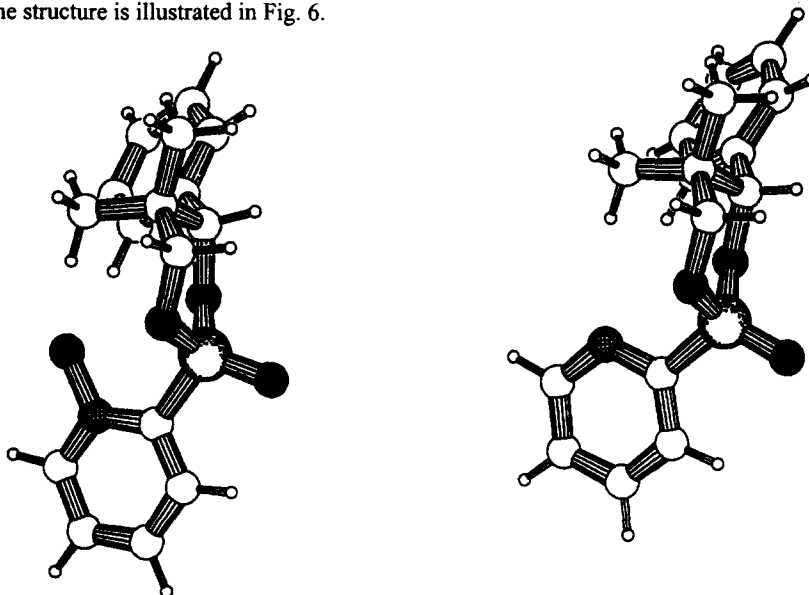


Fig. 6 RHF 3-21G/6-31G* optimized geometries of **10b** (left) and **12b** (right)

The dioxaphosphorinane ring retains its chair conformation with bond lengths and angles comparable to those found for **10a**. The energy calculated for this optimized geometry is higher than that of **10a** by 0.68 kcal/mol. The ^1H NMR and NOESY data are also in accord with a chair conformation. Both axial hydrogens show small couplings to phosphorus ($^3J_{\text{PH}}=2.2$ Hz) whereas the equatorial hydrogen has a large coupling ($J_{\text{PH}} = 22.0$ Hz). An “inward” conformation (Fig. 6) is also calculated for **12b**, which, however, has not been synthesized.

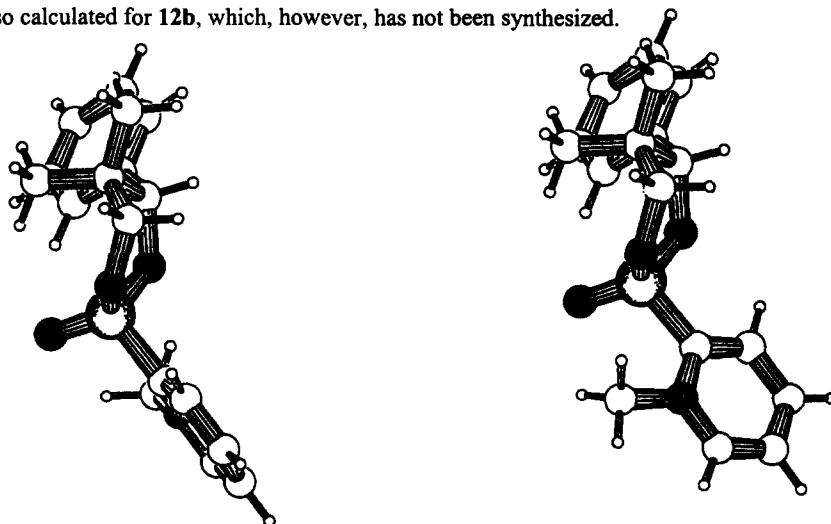


Fig. 7 RHF 3-21G/6-31G* optimized geometries of **13a**. Syn-(left) and anti-conformations (right).

The calculated structures of the N-methylated derivative **13a** is shown in Fig. 7. RHF calculations for **13a** reveal two minimal energy conformations, one with the N-methyl and phenyl groups on the same side of the molecule (*syn*), and the corresponding *anti*-conformation. Both calculated structures indicate a twist-boat conformation. This is not in agreement with the NMR data which indicate proton-phosphorus couplings constants $^3J_{\text{PH,ax}}=0$ Hz and $^3J_{\text{PH,eq}}=24.1$ Hz consistent with a chair conformation. The NMR data and calculated structures are in agreement, however, in that the N-methyl group is placed “outside” of the dioxaphosphorinane ring.

The ring deformation is probably caused by the strong electrostatic potential of the system owing to the bare positive charge. Intramolecular interaction of the electronegative oxygen atoms with the positive charge forces the endocyclic oxygen atoms towards the pyridinyl moiety, resulting in the calculated twist-boat conformer. In solution, the charge will be compensated by a counterion and by the solvent. To mimic computationally this as closely as viable, an iodide counter ion was included in the system. The initial position of the iodide relative to the pyridine ring was obtained from the optimized geometry of a model system, N-methylpyridinium iodide. Iodine was described at the 3-21G* basis level. The preliminary result is depicted in Fig. 8.

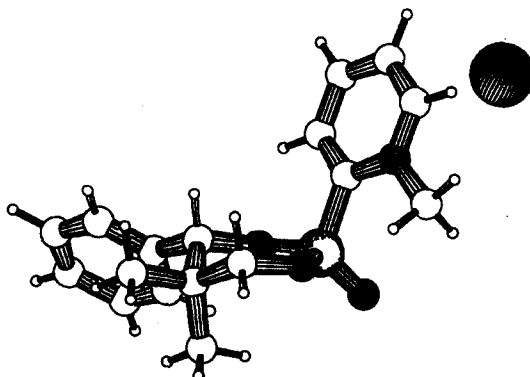


Fig. 8 Preliminary geometry of the *anti*-conformation of **13a** with counterion.

Although the dioxaphosphorinane ring is flattened at the phosphorus end, the chair-like conformation is retained.

Although a counterion has not been included in the calculations, both minimal energy conformations of **13b** (not prepared!) have normal chair conformations. This is best explained by the fact that deformation of the chair conformer in this case would lead to an *increase* in distance between the positively charged pyridyl moiety and the phosphorinane oxygens.

The RHF optimized geometries of 2-thia-1,3,2-dioxaphosphorinanes are shown in Fig. 9.

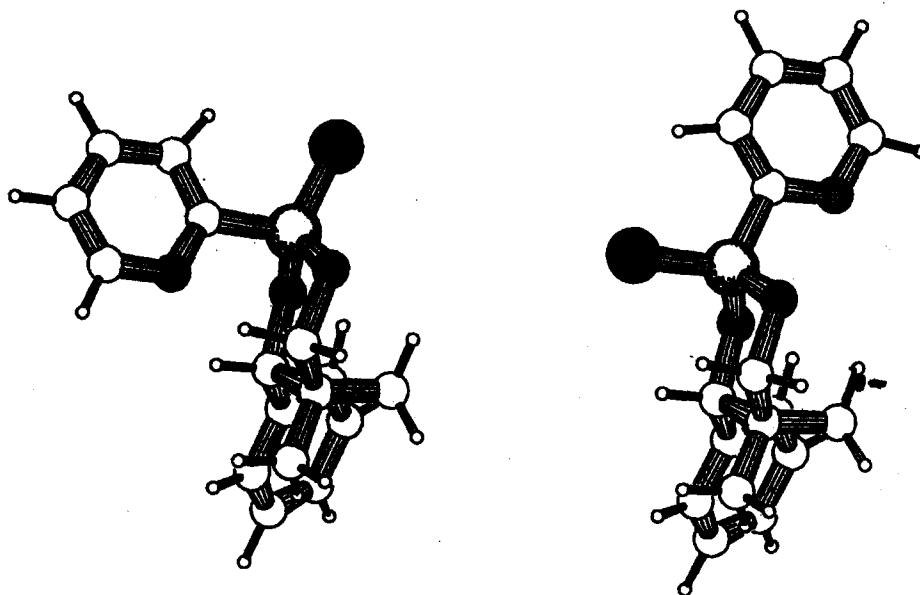


Figure 9. RHF 3-21G/6-31G* optimized geometries of 14a (left) and 14b (right)

Whereas the phosphoryl oxygen atom in 10b inclines towards the equatorial position, the corresponding sulfur atom in 14b adopts a nearly perfect axial disposition. The sulfur-phosphorus bond lengths are relatively long; P=S bond lengths are normally in the range of 1.92 Å.²⁹ A length of 1.950 Å is calculated for 14a and 1.983 Å for 14b. The greater P=S bond length for 14b can be explained by anomeric interactions between endocyclic oxygen lone pairs and the antibonding P-S sigma* orbital.³¹ Phosphorus-sulfur bond lengths are slightly smaller if sulfur is described at the 3-21 G* level (1.939 Å and 1.947 Å, respectively), again indicating the minor influence of BSSE on the optimized geometries.

Compound 11 (tetramethylated) is included because its NMR spectrum differed significantly. The resonance for the benzylic hydrogen is shifted to even lower field owing to close contact with the nitrogen atom, expected from orientation of the pyridinyl moiety towards the benzylic position to relieve repulsion imposed by the axial methyl group. The RHF calculations (Fig. 10) give a somewhat different picture.

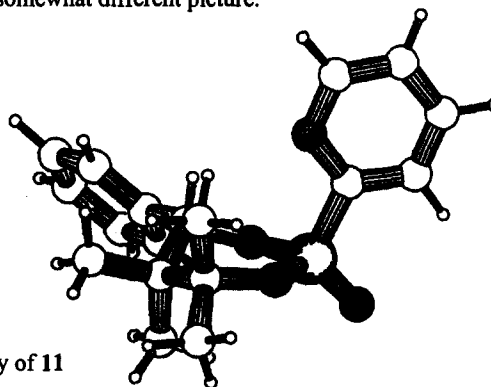


Fig. 10 RHF 3-21G/6-31G* optimized geometry of 11

These calculations indicate that strain is chiefly relieved by deformation of the dioxaphosphorinane ring, diminishing the difference between axial and equatorial methyl groups. The pyridinyl group is only slightly twisted out of plane; the dihedral angle defined by O1-P-C12-N is 175.4°, a value that compares closely with the corresponding angle in the X-ray structure of the N-oxide 12a. (174.3°). Although the diagnostic $^3J_{\text{PH}}$ coupling constants for axial and equatorial hydrogen atoms are not available in the ^1H NMR spectra of 14, the same trend is observed to a lesser extent in the $^4J_{\text{PC}}$ coupling constants for axial and equatorial methyl groups in ^{13}C NMR spectra. No coupling is observed for the axial methyl group, whereas the equatorial methyl group has a $^4J_{\text{PC}}$ coupling constant of 6.1 Hz. The value is significantly lower than observed for equatorial methyl groups in diphosphite-borane complexes and di(thio)phosphates (generally $^4J_{\text{PC}}=8.5\text{--}11$ Hz), consistent with the deviation from an ideal chair conformation.

Pertinent data for 10b, 12b, 13a,b, 15a,b and 11 are collected in Tables 2 and 3.^{32,33}

Tables 2 and 3

Table 2 RHF 3-21G/6-31G* geometrical data for 10b, 12b, and 13a

	10b	12b	13a-syn	13a-anti	13a-anti ^a
Energy (AU)	-1236.2067	-1310.9739	-1275.6158	-1275.6128	-
Bond lengths (Å)					
P1-O1	1.464	1.465	1.459	1.459	1.454
P1-O2	1.587	1.571	1.570	1.563	1.579
P1-O3	1.588	1.582	1.569	1.575	1.575
P1-C12	1.793	1.806	1.829	1.830	1.825
Bond angles (deg)					
O1-P1-O2	116.11	116.13	116.78	118.79	116.21
O1-P1-O3	115.64	115.14	118.56	116.43	116.06
O1-P1-C12	113.45	108.64	111.19	110.93	112.58
O2-P1-O3	102.13	103.40	103.55	103.57	103.98
O2-P1-C12	103.33	106.45	102.24	100.95	101.44
O3-P1-C12	104.58	106.33	102.41	104.17	104.61
Dihedral angles (deg)					
O1-P1-C12-N1	-174.33	-172.41	58.54	-58.46	-65.37
P1-O2-C1-C2	-49.39	-39.18	13.21	13.61	-39.01
P1-O3-C3-C2	56.43	63.71	32.68	33.39	32.33

^a Preliminary results of geometry optimization with iodide counter ion.

Table 3 RHF 3-21G/6-31G* geometrical data for 13b, 15a, 15b, and 11

	13b- <i>syn</i>	13b- <i>anti</i>	15a	15b	11
Energy (AU)	-1275.6149	-1275.5110	-1558.7397	-1558.7497	-1314.2710
Bond lengths (Å)					
P1-S1/O1	1.458	1.476	1.950	1.983	1.459
P1-O2	1.577	1.564	1.577	1.576	1.588
P1-O3	1.570	1.572	1.565	1.570	1.576
P1-C12	1.826	1.800	1.823	1.788	1.800
Bond angles (deg)					
O1-P1-O2	116.83	115.65	113.34	111.46	114.66
O1-P1-O3	118.49	113.24	115.86	112.28	115.78
O1-P1-C12	112.52	114.95	111.72	113.52	111.70
O2-P1-O3	103.34	105.73	105.03	103.85	102.76
O2-P1-C12	102.16	99.84	104.16	106.77	104.92
O3-P1-C12	101.16	106.06	105.74	108.37	105.95
Dihedral angles (deg)					
O1-P1-C12-N1	-58.10	73.15	173.60	178.53	175.36
P1-O2-C1-C2	-56.59	-52.73	-48.17	-56.68	-56.54
P1-O3-C3-C2	55.04	66.58	64.86	64.39	21.80

Conclusions

There can be little doubt that the pyridinyl-2-phosphonates described here strongly prefer a conformation with the pyridinyl nitrogen *anti* to the P=O double bond. The same is true of the N-oxide. The magnitude of this effect is revealed quite dramatically in 10a and 12a. We are not aware of previous demonstrations of this strong conformational preference.

One direct consequence of this effect is that it is difficult to prepare metal complexes of 10 and 12 wherein both pyridinyl nitrogen and phosphorus act in a bidentate fashion. Our experiences so far are in accord with this conclusion. Does this effect apply to all pyridinyl-2-phosphonates? Metal complexes of simpler (devoid of six-ring) ligands are known to complex various transition metals.⁵ It is therefore possible in such derivatives to achieve the desired *syn* arrangement of ligating sites. How great the energy price is, however, not at all clear. One should clearly be cognizant of this conformational preference in pyridinyl-2-phosphonates and take full account of the consequences. An interesting speculation is whether this conformational preference plays any role in the known insecticidal properties of compounds like 6.

General remarks

Optical rotations were measured on a Perkin-Elmer 241 polarimeter at room temperature. ¹H NMR spectra were taken on Varian Gemini-200 BB, VXR-300S or Unity-500 spectrometers at 200, 300 and 500 MHz, respectively. ¹³C and ¹H-decoupled ³¹P NMR spectra were recorded at 50.3 or 75.5 MHz and 81.0 or 121.4 MHz, respectively. ¹¹B NMR and ¹⁹F NMR spectra were recorded at 96.2 and 188 MHz, respectively. Chemical shift values are denoted in ppm and are referenced to residual protons in deuterated solvents for ¹H NMR (CDCl₃: 7.26 ppm; benzene-*d*₆: 7.16 ppm), to solvent resonances for ¹³C NMR (CDCl₃: 77.01 ppm; benzene-*d*₆: 128.0 ppm) to external (PhO)₃PO (-18.0 ppm) for ³¹P NMR, external BF₃•OEt₂ (0 ppm) for ¹¹B NMR and external CCl₄ (0 ppm) for ¹⁹F NMR. Mass spectra were

recorded on AEI-MS-902 (EI) and Ribermag R10-10C (CI) mass spectrometers operated by Mr. A. Kiewiet. Elemental analyses were performed by Mr. H. Draaijer, Mr. J. Ebels, and Mr. J. Hommes. Solvents were distilled prior to use (CHCl_3 , CH_2Cl_2 , Et_2O , toluene, pentane and hexanes from P_2O_5 , THF and benzene from Na/benzophenone).

Pyridine-*N*-methoxide methosulfate (**5**),⁹ pyridinyl-2-phosphonyl dichloride (**6**),^{9,12} and 1-phenyl-2,2-dimethylpropane-1,3-diol (**9**)^{13a} were synthesized according to literature procedures.

Restricted Hartree Fock calculations were performed in the Gaussian-94 package³² on Hewlett Packard 9000/735 machines. Initial conformations were generated on a CAChe system. Conformations were optimized at the HF/3-21G level for C, H, N, and O at the HF/3-21G* level for I, and the HF/6-31G* for P and S,³³ using the default Berny gradient minimization algorithms in Gaussian-94. Single point energies were calculated at the HF/6-31G* level for all atoms.

(*S*)-2H-2-Oxo-5,5-dimethyl-4-(*R*)-phenyl-1,3,2-dioxaphosphorinane (8**)**

A solution of H_3PO_3 (4.55 g, 55.5 mmol) in 55 mL of THF was added all at once to a solution of dicyclohexylcarbodiimide (23.0 g, 0.11 mmol) and (*R*)-(-)-**9** (10.0 g, 55.5 mmol) in 165 mL of THF. In an exothermic reaction a white precipitate of dicyclohexylurea was formed. After stirring at room temperature for 30 min, the flask was sonicated for 1 h. The solids were removed by filtration and washed three times with ether. The combined filtrates were evaporated to give an off-white solid. ¹H NMR spectroscopy revealed the presence of both epimers of **8**. Crystallization from toluene/ether afforded the 2*S*,4*R* epimer exclusively, as colorless crystals. Yield: 7.02 g, 31 mmol, 56%.

Spectroscopic data of the product were in accordance with those previously reported.¹⁶

(*S*)-(-)-and(*R*)-(+)-2-(2-Pyridinyl)-2-oxo-5,5-dimethyl-4-(*R*)-phenyl-1,3,2-dioxaphosphorinanes (10a** and **b**)**

Method A.

To an ice-cooled solution of (*R*)-(-)-**9** (5.59 g, 31.0 mmol) and Et_3N (10 mL, 7.3 g, 72 mmol) in 25 mL of chloroform was added dropwise **6** (6.25 g, 34.7 mmol) in 5 mL of chloroform. The resulting suspension was stirred overnight at room temperature. The reaction mixture was washed with 1N HCl solution and the aqueous layer was extracted three times with CHCl_3 . The combined organic layers were washed with brine, dried over Na_2SO_4 and concentrated. The brown viscous oil contained both epimers of **10** in a 1:1 ratio (¹H NMR). Column chromatography (silica gel, EtOAc) and subsequent crystallization from EtOAc/hexanes afforded 3.45 g (11.4 mmol, 37%) of **10a** and 2.27 g (7.46 mmol, 24%) of **10b** as white crystalline solids.

Method B

To an ice-cooled solution of (*R*)-(-)-**8** (1.26 g, 5.57 mmol) and *t*-BuOK (0.63 g, 5.61 mmol) in 10 mL of THF was added **5** (1.25 g, 5.65 mmol) in THF (25 mL). The resulting suspension was stirred overnight. Saturated aqueous NH_4Cl was added and the organic layer was separated. The aqueous layer was extracted twice with CHCl_3 . The combined organic layers were washed with brine, dried over Na_2SO_4 and evaporated to give an oil. The epimers **10a,b**

were present in a 6:1 ratio as determined by ^1H NMR spectroscopy. Column chromatography (silica gel, EtOAc) gave a colorless oil. Trituration with hexanes afforded **10a** as a white crystalline material (0.93 g, 3.05 mmol, 55%). (*S,R*)-(-)-**10a**:

$R_f = 0.55$. $[\alpha]_{578} -129.5$ ($c = 0.498$, CHCl_3). ^1H NMR (CDCl_3): δ 8.75 (m, 1H, $\text{C}_5\text{H}_4\text{N}$); 8.03 (m, 1H, $\text{C}_5\text{H}_4\text{N}$); 7.81 (m, 1H, $\text{C}_5\text{H}_4\text{N}$); 7.44 (m, 1H, $\text{C}_5\text{H}_4\text{N}$); 7.38-7.31 (m, 5H, C_6H_5); 5.90 (s, 1H, CHPh); 4.96 (d, $^2J_{AB} = 10.6$ Hz, 1H, CH_2); 4.08 (dd, $^2J_{AB} = 10.6$ Hz, $^3J_{PH} = 21.2$ Hz, 1H, CH_2); 1.19 (s, 3H, CH_3); 0.87 (s, 3H, CH_3); ^{13}C NMR (CDCl_3): δ 153.39 (d, $J_{PC} = 220.7$ Hz, $\text{C}_5\text{H}_4\text{N}$); 149.68 (d, $J_{PC} = 23.4$ Hz, $\text{C}_5\text{H}_4\text{N}$); 136.16 (d, $J_{PC} = 11.7$ Hz, $\text{C}_5\text{H}_4\text{N}$); 135.98 (C_{qPh}); 128.21 (CH_{Ph}); 127.96 (d, $J_{PC} = 25.4$ Hz, $\text{C}_5\text{H}_4\text{N}$); 127.66 (CH_{Ph}); 127.28 (CH_{Ph}); 126.08 (d, $J_{PC} = 3.9$ Hz, $\text{C}_5\text{H}_4\text{N}$); 88.74 (d, $J_{PC} = 7.8$ Hz, CH); 79.77 (d, $J_{PC} = 5.9$ Hz, CH_2); 36.83 (d, $J_{PC} = 5.9$ Hz, C_q); 21.13 (CH_3); 17.37 (CH_3); ^{31}P NMR (CDCl_3): δ 1.9. Anal. Calcd for $\text{C}_{16}\text{H}_{18}\text{NO}_3\text{P}$: C, 63.36; H, 5.98; N, 4.62; P, 10.21. Found: C, 63.25; H, 5.93; N, 4.61; P, 10.11. HRMS calcd 303.102, found 303.102.

^1H NMR (C_6D_6): δ 8.31 (m, 1H, 6- $\text{C}_5\text{H}_4\text{N}$); 8.10 (m, 1H, 3- $\text{C}_5\text{H}_4\text{N}$); 7.19 (m, 2H, C_6H_5); 7.03 (m, 3H, C_6H_5); 6.84 (m, 1H, 4- $\text{C}_5\text{H}_4\text{N}$); 6.50 (m, 1H, 5- $\text{C}_5\text{H}_4\text{N}$); 6.03 (s, 1H, CHPh); 4.93 (d, $^2J_{AB} = 10.74$ Hz, 1H, CH_2); 3.67 (dd, $^2J_{AB} = 10.75$ Hz, $^3J_{PH} = 21.0$ Hz, 1H, CH_2); 1.04 (s, 3H, CH_3); 0.35 (s, 3H, CH_3).

(R,R)-(+)-10b:

$R_f = 0.44$; $[\alpha]_{578} +46.6$ ($c = 0.498$, CHCl_3); ^1H NMR (CDCl_3): δ 8.90 (m, 1H, $\text{C}_5\text{H}_4\text{N}$); 8.16 (m, 1H, $\text{C}_5\text{H}_4\text{N}$); 7.85 (m, 1H, $\text{C}_5\text{H}_4\text{N}$); 7.51 (m, 1H, $\text{C}_5\text{H}_4\text{N}$); 7.37-7.31 (m, 5H, C_6H_5); 5.64 (d, $^3J_{PH} = 2.2$ Hz, 1H, CHPh); 4.66 (dd, $^2J_{AB} = 11.4$ Hz, $^3J_{PH} = 2.2$ Hz, 1H, CH_2); 4.05 (dd, $^2J_{AB} = 11.4$ Hz, $^3J_{PH} = 22.0$ Hz, 1H, CH_2); 1.25 (s, 3H, CH_3); 0.88 (s, 3H, CH_3); ^{13}C NMR (CDCl_3): δ 150.72 (d, $J_{PC} = 24.4$ Hz, $\text{C}_5\text{H}_4\text{N}$); 149.83 (d, $J_{PC} = 236.8$ Hz, $\text{C}_5\text{H}_4\text{N}$); 136.01 (C_{qPh}); 135.99 (d, $J_{PC} = 13.43$ Hz, $\text{C}_5\text{H}_4\text{N}$); 129.00 (d, $J_{PC} = 26.9$ Hz, $\text{C}_5\text{H}_4\text{N}$); 128.27 (CH_{Ph}); 127.71 (CH_{Ph}); 127.33 (CH_{Ph}); 126.64 (d, $J_{PC} = 4.9$ Hz, $\text{C}_5\text{H}_4\text{N}$); 85.13 (d, $J_{PC} = 6.1$ Hz, CH); 75.98 (d, $J_{PC} = 6.1$ Hz, CH_2); 36.50 (d, $J_{PC} = 3.7$ Hz, C_q); 21.68 (CH_3); 17.44 (CH_3); ^{31}P NMR (CDCl_3): δ 9.8. Anal. Calcd for $\text{C}_{16}\text{H}_{18}\text{NO}_3\text{P}$: C, 63.36; H, 5.98; N, 4.62; P, 10.21. Found: C, 63.40; H, 5.91; N, 4.56; P, 10.14. HRMS calcd 303.102, found 303.102.

^1H NMR (C_6D_6): δ 8.50 (m, 1H, 6- $\text{C}_5\text{H}_4\text{N}$); 8.23 (m, 1H, 3- $\text{C}_5\text{H}_4\text{N}$); 7.22 (m, 2H, C_6H_5); 7.04 (m, 3H, C_6H_5); 6.81 (m, 1H, 4- $\text{C}_5\text{H}_4\text{N}$); 6.48 (m, 1H, 5- $\text{C}_5\text{H}_4\text{N}$); 5.43 (d, $^3J_{PH} = 2$ Hz, 1H, CHPh); 4.35 (dd, $^2J_{AB} = 11$ Hz, $^3J_{PH} = 2$ Hz, 1H, CH_2); 3.58 (dd, $^2J_{AB} = 11$ Hz, $^3J_{PH} = 22$ Hz, 1H, CH_2); 1.27 (s, 3H, CH_3); 0.25 (s, 3H, CH_3).

Resolution of 3-hydroxy-2,2-dimethylpropionic acid

To a suspension of racemic 3-hydroxy-2,2-dimethylpropionic acid (151 g, 0.78 mol) in water (2.5 L) was added (-)- α -methyl benzylamine (110 mL, 103 g, 0.85 mol). The suspension was heated to reflux until a clear, yellow solution was obtained. Upon cooling to room temperature a white precipitate of the *n*-salt formed, which was collected by filtration. The filtrate was made basic, washed with ether to remove (-)- α -methyl benzylamine, and acidified to give the (-)-acid. The combined acid portions from the first two crystallizations were collected (68.8 g, 0.35 mol), resuspended in water and (+)- α -methyl benzylamine (48 mL, 45.1 g, 0.37 mol) was added. Both *n*-salts were recrystallized from water until the optical rotation was constant at $[\alpha]_{578} \pm 13.9$ ($c = 1$, MeOH). Usually this required three crystallizations. Since optical rotation was found to be an unreliable measure for the enantiomeric purity of the salts, at this point samples of the salts were converted to the esters for HPLC analysis. Basification, washing with

ether, acidification and filtration afforded the acids as white solids.

Yield 34.8 g (0.18 mol, 23%). (*S*)-(+)-enantiomer: 54.4 g, 0.28 mol, 36%.

Acids and amines from mother liquors were recovered.

Enantiomerically pure ethyl 3-hydroxy-2,2-dimethylpropionates

A suspension of (*R*)-(-)-3-hydroxy-2,2-dimethylpropionic acid (44.5 g, 0.24 mol) in ethanol was refluxed overnight with a catalytic amount of sulfuric acid. The resulting clear solution was cooled to room temperature, neutralized with saturated NaHCO₃ solution, and concentrated. The mixture was taken up in ether/water. The organic layer was separated and the water layer was extracted twice with ether. The combined organic layers were washed with dilute aqueous NaOH, saturated aqueous NH₄Cl and brine. Drying over Na₂SO₄, evaporation of the solvent, and bulb-to-bulb distillation under reduced pressure afforded (*R*)-(+)-ester (47.9 g, 0.22 mol, 94%) as a colorless oil; bp 100 °C/0.01 mm Hg.

(*R*)-(+)-ester: $[\alpha]_{578}^0$ (c = 1.14, MeOH); $[\alpha]_{365}^0 + 17.6$ (c = 1.05, MeOH). HPLC: (Chiralpak AD) $R_f = 10.6$ min.

(*S*)-(-)-ester: $[\alpha]_{365}^0 - 17.7$ (c = 1.14, MeOH). HPLC: (Chiralpak AD) $R_f = 9.2$ min.

(*R*)-(-)-1-Phenyl-2,2,3-trimethylbutane-1,3-diol

A 0.95 M solution of MeMgI in ether (360 mL, 0.34 mol) was added dropwise to an ice-cooled solution of (*R*)-(+)-ethyl 3-hydroxy-2,2-dimethylpropionate (23.4 g, 0.105 mol) in THF (50 mL). A white precipitate formed immediately and methane was liberated. The suspension was stirred at room temperature overnight and carefully neutralized with saturated NH₄Cl solution. The organic layer was separated and the water layer was extracted twice with ether. The combined organic layers were washed with saturated Na₂S₂O₅ solution, brine, dried over Na₂SO₄, and evaporated. The slightly yellow oil was crystallized from hexanes to give the product as white needles; yield 16.3 g (78 mmol, 74%); mp 117.7–119.0 °C; $[\alpha]_{578}^0 - 36.7$ (c = 0.505, CHCl₃); ¹H NMR (CDCl₃): δ 7.33 (m, 5H, C₆H₅); 4.95 (s, 1H, CH); 4.05 (s, 1H, OH); 3.44 (s, 1H, OH); 1.44 (s, 3H, CH₃); 1.22 (s, 3H, CH₃); 0.95 (s, 3H, CH₃); 0.64 (s, 3H, CH₃); ¹³C NMR (CDCl₃): δ 141.63 (C_{qAr}); 127.49 (CH_{Ar}); 127.38 (CH_{Ar}); 127.32 (CH_{Ar}); 79.62 (CH); 77.34 (C_q); 43.13 (C_q); 26.56 (CH₃); 25.39 (CH₃); 22.82 (CH₃); 14.57 (CH₃). Anal. Calcd for C₁₃H₂₀O₂: C, 74.96; H, 9.68. Found: C, 75.02; H, 9.63. $[M+H]^+ = 209$ (CI; NH₃). HPLC (Chiralpak OD): $R_f = 17.8$ min.

The other enantiomer was obtained in the same way starting from (*S*)-(-)-ester; $[\alpha]_{578}^0 + 37.1$ (c = 0.51, CHCl₃). HPLC (Chiralpak OD): $R_f = 15.9$ min.

(*S*)-(+)-2-(2-Pyridinyl)-2-oxo-4,4,5,5-tetramethyl-6-(*S*)-phenyl-1,3,2-dioxaphosphorinane (11a)

This compound was prepared analogously to 10a from 6 and (*S*)-(+)-1-phenyl-2,2,3-trimethylbutane-1,3-diol and purified by means of column chromatography (silica gel, EtOAc). Compound 11a was obtained as a white solid in 24% yield.

$R_f = 0.5$; $[\alpha]_{365}^0 + 65.0$ (c = 0.408, CHCl₃); ¹H NMR (CDCl₃): δ 8.71 (m, 1H, C₅H₄N); 8.01 (m, 1H, C₅H₄N); 7.74 (m,

1H, C₅H₄N); 7.47-7.44 (m, 2H, C₆H₅); 7.39-7.29 (m, 4H, C₆H₅, C₅H₄N); 6.16 (s, 1H, CHPh); 1.65 (s, 3H, CH₃); 1.48 (d, ¹J_{PH} = 1.8 Hz, 3H, CH₃); 1.25 (s, 3H, CH₃); 0.79 (s, 3H, CH₃); ¹³C NMR (CDCl₃): δ 153.86 (d, ¹J_{PC} = 228.3 Hz, C₅H₄N); 149.83 (d, J_{PC} = 24.4 Hz, C₅H₄N); 136.60 (d, J_{PC} = 8.6 Hz, C₅H₄N); 135.85 (d, J_{PC} = 12.2 Hz, C_{qPh}); 128.11 (CH_{Ph}); 128.01 (d, J_{PC} = 25.6 Hz, C₅H₄N); 127.58 (CH_{Ph}); 125.67 (d, J_{PC} = 4.9 Hz, C₅H₄N); 90.89 (d, J_{PC} = 8.6 Hz, C_q); 84.52 (d, J_{PC} = 5.8 Hz, CH); 42.20 (d, J_{PC} = 6.1 Hz, C_q); 26.21 (d, J_{PC} = 6.1 Hz, CH₃); 25.18 (CH₃); 21.96 (CH₃); 15.83 (CH₃); ³¹P NMR (CDCl₃): δ 1.7. Anal. Calcd for C₁₈H₂₂NO₃P: C, 65.25; H, 6.69; N, 4.23; P, 9.35. Found: C, 65.22; H, 6.61; N, 4.17; P, 9.21. HRMS calcd 331.134, found 331.134.

2-(R)-(2-Pyridinyl)-2-oxo-5,5-dimethyl-4-(R)-phenyl-1,3,2-dioxaphosphorinane-N-oxide (12)

A solution of 0.63 g (2.07 mmol) of **10a** in 5 mL of acetic acid and 1 mL of 30% H₂O₂ in H₂O was warmed at 40 °C for 48 h. The solution was concentrated on the rotary evaporator, diluted with water and concentrated. The residue was taken up in CHCl₃ and washed with saturated aqueous NaHCO₃. The aqueous solution was extracted with CHCl₃. The combined organic layers were washed with brine, dried over Na₂SO₄, and evaporated. The yellowish solid was recrystallized from toluene/hexanes to afford **12** as off-white needles; yield 0.39 g (1.22 mmol; 59%). Another recrystallization from the same solvent mixture afforded **12** as white needles,

mp 188.5-188.6 °C (dec.); [α]_D²⁵ -54.2 (c = 1, CHCl₃). ¹H NMR (CDCl₃): δ 8.13 (m, 2H, C₅H₄N); 7.34 (m, 7H, C₆H₅, C₅H₄N); 6.17 (s, 1H, CHPh); 5.17 (d, ²J_{AB} = 10.0 Hz, 1H, CH₂); 4.07 (dd, ²J_{AB} = 10.0 Hz, ³J_{PH} = 21.5 Hz, 1H, CH₂); 1.21 (s, 3H, CH₃); 0.83 (s, 3H, CH₃); ¹³C NMR (CDCl₃): δ 141.93 (d, ¹J_{PC} = 216 Hz, C₅H₄N); 139.15 (d, J_{PC} = 6.1 Hz, C₅H₄N); 136.11 (d, J_{PC} = 8.5 Hz, C_{qPh}); 133.98 (d, J_{PC} = 12.2 Hz, C_{qPh}); 128.78 (CH_{Ph}); 128.25 (CH_{Ph}); 127.70 (CH_{Ar}); 127.57 (CH_{Ar}); 125.39 (d, J_{PC} = 11.0 Hz, C₅H₄N); 90.80 (d, J_{PC} = 7.3 Hz, CH); 81.34 (d, J_{PC} = 6.1 Hz, CH₂); 36.85 (d, J_{PC} = 8.5 Hz, C_q); 21.19 (CH₃); 18.05 (CH₃); ³¹P NMR (CDCl₃): δ -2.6. Anal. Calcd for C₁₆H₁₈NO₄P: C, 60.19; H, 5.68; P, 9.70. Found: C, 60.06; H, 5.70; P, 9.59. HRMS calcd 319.097, found 319.097.

¹H NMR (C₆D₆): δ 8.06 (m, 1H, 6-C₅H₄N); 7.41 (m, 1H, 3-C₅H₄N); 7.27 (m, 2H, C₆H₅); 7.02 (m, 3H, C₆H₅); 6.46 (s, 1H, CHPh); 6.05 (m, 1H, 5-C₅H₄N); 5.95 (m, 1H, 4-C₅H₄N); 5.38 (d, ²J_{AB} = 9.77 Hz, 1H, CH₂); 3.74 (dd, ²J_{AB} = 9.77 Hz, ³J_{PH} = 21.0 Hz, 1H, CH₂); 1.15 (s, 3H, CH₃); 0.36 (s, 3H, CH₃).

N-Methyl-2-(R)-(2-pyridinyl)-2-oxo-5,5-dimethyl-4-(R)-phenyl-1,3,2-dioxaphosphorinane trifluoromethanesulfonate (13)

A solution of **10a** (130.7 mg, 0.43 mmol) and CF₃SO₃Me (52 microL, 75.4 mg, 0.46 mmol) in CH₂Cl₂ was stirred at room temperature for several days. After evaporation of the volatiles, the product was dissolved in methanol and precipitated by addition of ether. The white solid was collected by filtration; yield 119 mg (0.25 mmol, 59%); ¹H NMR (500 MHz; CDCl₃): δ 8.95 (m, 1H, 6-C₅H₄N); 8.52 (m, 1H, 4-C₅H₄N); 8.28 (m, 1H, 3-C₅H₄N); 8.13 (m, 1H, 5-C₅H₄N); 7.41 (m, 5H, C₆H₅); 5.84 (s, 1H, CHPh); 4.84 (d, ²J_{AB} = 11.1 Hz, 1H, CH₂); 4.58 (s, 3H, N-CH₃); 4.22 (dd, ²J_{AB} = 11.1 Hz, ³J_{PH} = 24.1 Hz, 1H, CH₂); 1.21 (s, 3H, CH₃); 0.83 (s, 3H, CH₃); ¹³C NMR (CDCl₃): δ 149.82 (d, J_{PC} = 7.3 Hz, C₅H₄N); 146.48 (d, ¹J_{PC} = 188.0 Hz, C₅H₄N); 145.53 (d, J_{PC} = 9.8 Hz, C₅H₄N); 134.24 (d, J_{PC} = 8.5 Hz, C₅H₄N); 132.33 (d, J_{PC} = 11.0 Hz, C₅H₄N); 130.60 (C_{qAr}); 129.11 (CH_{Ar}); 128.13 (CH_{Ar}); 127.56 (CH_{Ar}); 120.39 (q, J_{FC} = 320 Hz, CF₃); 90.28 (d, J_{PC} = 7.3 Hz, CH); 80.60 (d, J_{PC} = 7.3 Hz, CH₂); 48.85 (d, J_{PC} = 2.4 Hz, NCH₃); 36.92

(d, $J_{PC} = 6.1$ Hz, C_q); 20.33 (CH₃); 17.35 (CH₃); ³¹P NMR (CDCl₃): δ -6.4. ¹⁹F NMR (CDCl₃): δ -79.9. Anal. Calcd for C₁₈H₂₁F₃NO₆PS: C, 46.26; H, 4.53. Found: C, 46.14; H, 4.32.

2-(R)-(2-Pyridinyl)-2-thio-5,5-dimethyl-4-(R)-phenyl-1,3,2-dioxaphosphorinane (15a)

A toluene solution of **10a** (109.4 mg, 0.361 mmol) and Lawesson's reagent (72.9 mg, 0.18 mmol) was refluxed for 4 h. The reaction mixture was cooled to room temperature and stirred with 3 mL of 1N NaOH solution. The organic layer was separated and the aqueous layer was extracted twice with toluene. The combined organic layers were washed with brine, dried over Na₂SO₄ and concentrated. The resulting white solid was recrystallized from toluene/hexanes to afford **15a** as white crystals. Yield: 81.0 mg, 0.254 mmol, 70%;

¹H NMR (CDCl₃): δ 8.75 (m, 1H, C₅H₄N); 8.14 (m, 1H, C₅H₄N); 7.81 (m, 1H, C₅H₄N); 7.45-7.31 (m, 6H, C₆H₅, C₅H₄N); 5.74 (d, ³J_{PH} = 1.2 Hz, 1H, CHPh); 4.80 (dd, ²J_{AB} = 11 Hz, ³J_{PH} = 4 Hz, 1H, CH₂); 3.99 (dd, ²J_{AB} = 11 Hz, ³J_{PH} = 25 Hz, 1H, CH₂); 1.22 (s, 3H, CH₃); 0.87 (s, 3H, CH₃); ¹³C NMR (CDCl₃): δ 157.02 (d, $J_{PC} = 170.91$ Hz, C₅H₄N); 149.27 (d, $J_{PC} = 20.8$ Hz, C₅H₄N); 136.52 (d, $J_{PC} = 13.4$ Hz, C₅H₄N); 136.06 (d, $J_{PC} = 7.3$ Hz, C_{qPh}); 128.32 (CH_{Ph}); 127.84 (d, $J_{PC} = 29.3$ Hz, C₅H₄N); 127.77 (CH_{Ph}); 127.54 (CH_{Ph}); 126.64 (d, $J_{PC} = 3.7$ Hz, C₅H₄N); 89.30 (d, $J_{PC} = 9.8$ Hz, CH); 79.88 (d, $J_{PC} = 8.5$ Hz, CH₂); 36.79 (d, $J_{PC} = 6.1$ Hz, C_q); 21.43 (CH₃); 17.90 (CH₃); ³¹P NMR (CDCl₃): δ 70.6. Anal. Calcd for C₁₆H₁₈NO₂PS: C, 60.17; H, 5.68; N, 4.39. Found: C, 60.45; H, 5.67; N, 4.42. HRMS calcd 319.080, found 319.080.

2-(S)-(2-Pyridinyl)-2-thio-5,5-dimethyl-4-(R)-phenyl-1,3,2-dioxaphosphorinane (15b)

This compound was prepared analogously to **15a** from **10b** (111.2 mg, 0.367 mmol) and Lawesson's reagent (74.1 mg, 0.182 mmol) to give 58.2 mg (0.182 mmol, 50%) of **15b** as white crystals;

¹H NMR (CDCl₃): δ 8.90 (m, 1H, C₅H₄N); 8.34 (m, 1H, C₅H₄N); 7.88 (m, 1H, C₅H₄N); 7.50 (m, 1H, C₅H₄N); 7.33-7.28 (m, 5H, C₆H₅); 5.73 (d, ³J_{PH} = 4 Hz, 1H, CHPh); 4.83 (d, ²J_{AB} = 10.7 Hz, 1H, CH₂); 3.99 (dd, ²J_{AB} = 10.7 Hz, ³J_{PH} = 23.0 Hz, 1H, CH₂); 1.20 (s, 3H, CH₃); 0.81 (s, 3H, CH₃); ¹³C NMR (CDCl₃): δ 153.24 (d, $J_{PC} = 196.7$ Hz, C₅H₄N); 150.53 (d, $J_{PC} = 22.9$ Hz, C₅H₄N); 136.28 (d, $J_{PC} = 13.7$ Hz, C₅H₄N); 135.92 (d, $J_{PC} = 9.5$ Hz, C_{qPh}); 128.26 (CH_{Ph}); 128.18 (d, $J_{PC} = 31.7$ Hz, C₅H₄N); 127.71 (CH_{Ph}); 127.57 (CH_{Ph}); 126.56 (d, $J_{PC} = 3.8$ Hz, C₅H₄N); 84.06 (d, $J_{PC} = 5.3$ Hz, CH); 75.09 (d, $J_{PC} = 5.7$ Hz, CH₂); 37.54 (d, $J_{PC} = 3.4$ Hz, C_q); 21.56 (CH₃); 17.74 (CH₃); ³¹P NMR (CDCl₃): δ 79.9. HRMS calcd 319.080, found 319.080.

2-(R)-(2-Pyridinyl)-2-oxo-5,5-dimethyl-4-(R)-phenyl-1,3,2-dioxaphosphorinane borane adduct (14)

To an ice-cooled solution of 0.51 g (1.68 mmol) of **10a** in 10 mL of THF was added 3 mL of 0.7 M (2.1 mmol) BH₃·THF in THF. After several minutes a white precipitate formed. The suspension was stirred at room temperature for another hour. The product was separated from the supernatant by centrifugation, washed three times with 5 mL portions of ether, and dried *in vacuo* to afford **14** as a white solid; yield 0.32 g (1.01 mmol; 60%); ¹H NMR (C₆D₆): δ 8.46 (m, 1H, 3-C₅H₄N); 8.35 (m, 1H, 6-C₅H₄N); 7.29 (m, 2H, Ph); 7.03 (m, 3H, Ph); 6.48 (m, 1H, 4-C₅H₄N); 6.10 (d, ³J_{PH} = 2.4 Hz, 1H, CHPh); 5.99 (m, 1H, 5-C₅H₄N); 5.13 (dd, ²J_{AB} = 10.3 Hz, ³J_{PH} = 1.5 Hz, 1H, CH₂); 3.74 (dd, ²J_{AB} = 10.3 Hz, ³J_{PH} = 18.1 Hz, 1H, CH₂); 3.56 (d, $J = 130$ Hz, 3H, BH₃); 1.25 (s, 3H, CH₃); 0.30 (s, 3H, CH₃); ¹³C

NMR (CDCl₃): δ 151.47 (d, $J_{PC} = 12.2$ Hz, C H N); 139.35 (d, $J_{PC} = 11.0$ Hz, C H N); 135.49 (d, $J_{PC} = 7.3$ Hz, C₅H₄N); 133.82 (d, $J_{PC} = 15.9$ Hz, C₅H₄N); 128.61 (CH_{Ph}); 127.95 (CH_{Ph}); 127.64 (CH_{Ph}); 89.73 (d, $J_{PC} = 7.3$ Hz, CH); 79.22 (d, $J_{PC} = 6.1$ Hz, CH₂); 37.22 (d, $J_{PC} = 8.5$ Hz, C_q); 21.72 (CH₃); 18.50 (CH₃); ³¹P NMR (C₆D₆): δ -1.7; ¹¹B NMR (CDCl₃): δ -10.9.

Molecular structures of 2-(R)-(2-pyridinyl)-2-oxo-5,5-dimethyl-4-(R)-phenyl-1,3,2-dioxaphosphorinane (10a) and 2-(R)-(2-pyridinyl)-2-oxo-5,5-dimethyl-4-(R)-phenyl-1,3,2-dioxaphosphorinane-N-oxide (12)

Crystals of **10a** and **12** were obtained from saturated solutions of the respective compounds in toluene/hexanes. Crystal structure determination for **10a**: C₁₆H₁₈NO₄P, $M_r = 303.30$, colorless, block-shaped crystal (0.2 x 0.2 x 0.5 mm), orthorhombic $P2_12_1$, (no. 19), with: $a = 8.8425(7)$, $b = 11.4530(6)$, $c = 30.7161(6)$ Å, $V = 3110.7(3)$ Å³, $Z = 8$, $D = 1.2952(1)$ g cm⁻³, $\mu(\text{Mo K}\alpha) = 1.9$ cm⁻¹, 6629 reflections measured, 5703 independent, $R_{\text{int}} = 0.0557$, ($0.66^\circ < \theta < 25.37^\circ$), ω scan, $T = 150$ K, Mo K α radiation, graphite monochromator ($\lambda = 0.71073$ Å) on an Enraf-Nonius CAD 4 Turbo diffractometer on rotating anode. Data were corrected for Lp effects and for linear instability of the reference reflections, but not for absorption. The structure was solved by automated direct methods (SHELXS86). Refinement on F^2 was carried out by full-matrix least-squares techniques (SHELXL-93); no observance criterium was applied during refinement. Refinement converged at a final $wR2$ value of 0.1407. $R1 = 0.0739$ (for 3167 reflections with $F_o > 4\sigma(F_o)$) $S = 1.030$ for 383 parameters. Hydrogen atoms were included in the refinement on calculated positions riding on their carrier atoms. The Flack x parameter amounted to 0.14(19), indicating the assignment of the correct absolute structure. Refinement of the inverted structure resulted in slightly higher R-values and a Flack x parameter of 0.86(19). A final difference Fourier showed no residual density outside -0.26 and 0.27 e Å⁻³.

Crystal structure determination of **12a**: The same general procedure was followed as described for compound **10a**: C₁₆H₁₈NO₄P, $M_r = 316.30$, colorless, block-shaped crystal (0.2 x 0.2 x 0.6 mm, cut from from a larger aggregate), orthorhombic, space group $P2_12_1$, (no. 19) with $a = 6.5558(5)$, $b = 9.6092(7)$, $c = 24.615(2)$ Å, $V = 1550.6(2)$ Å³, $Z = 4$, $D = 1.3678(2)$ g cm⁻³, $\mu(\text{Mo K}\alpha) = 1.9$ cm⁻¹, 2083 reflections measured, 2057 independent, ($1.7^\circ < \theta < 27.5^\circ$). Refinement converged at a final $wR2$ value of 0.1185, $R1 = 0.0498$ (for 1619 reflections with $F_o > 4\sigma(F_o)$) $S = 1.087$, for 271 parameters. Hydrogen atoms were located on a difference Fourier map and their coordinates and temperature factors were refined. The Flack x parameter refined to -0.2(2). A final difference Fourier showed no residual density outside -0.60 and 0.31 e Å⁻³. Atomic coordinates, bond lengths and angles and thermal parameters for both structural determinations have been deposited at the Cambridge Crystallographic Data Centre.

Acknowledgement

This research was supported in part by a grant from the Netherlands Organization for Scientific Research (N.W.O.) administered by the Office for Chemical Research (S.O.N.) to A.C.D.

References:

1. Lobana, T.S. in *The Chemistry of Organophosphorus Compounds*, Vol. 2, Hartley, F.R., Ed. Wiley: Chichester, England 1992, and references cited therein.
2. Nicol, M.J.; Fleming, C.A.; Preston, J.S. in *Comprehensive Coordination Chemistry*, Vol. 6, Wilkinson, G.; Gillard, R.D.; McCleverty, J.A., Eds., Pergamon Press: Oxford 1987, Chapter 63, and references cited therein.
3. See for example: Conary, G.S.; Meline, R.L.; Schaeffer, R.; Duesler, E.N.; Paine, R.T., *Inorg. Chim. Acta* **1992**, 201, 165.
4. See for example: Caudle, L.J.; Duesler, E.N.; Paine, R.T. *Inorg. Chem.* **1985**, 24, 4441.
5. (a) McCabe, D.J.; Russell, A.A.; Karthikeyan, S.; Paine, R.T.; Ryan, R.R.; Smith, B. *Inorg. Chem.* **1987**, 26, 1230. (b) Conary, G.S.; Russell, A.A.; Paine, R.T.; Hall, J.H.; Ryan, R.R. *Inorg. Chem.* **1988**, 27, 3242. (c) Rapko, B.M.; Duesler, E.N.; Smith, P.H.; Paine, R.T.; Ryan, R.R. *Inorg. Chem.* **1993**, 32, 2164.
6. (a) Damiano, J.-P.; Munyejabo, V.; Postel, M. *Polyhedron* **1995**, 14, 1229, (b) Guillaume, p.; Postel, M. *Inorg. Chim. Acta* **1995**, 233, 109.
7. Wood, F.E.; Olmstead, M.M.; Farr, J.P.; Balch, A.L. *Inorg. Chim. Acta* **1985**, 97, 77.
8. (a) Specca, A.N.; Karayannis, N.M.; Pytlewski, L.L. *Inorg. Chim. Acta* **1972**, 6, 639. (b) Specca, A.N.; Mink, R.; Karayannis, N.M.; Pytlewski, L.L.; Owens, C. *J. Inorg. Nucl. Chem.* **1973**, 35, 1833. (c) Brill, T.B.; Landon, S.J. *Chem. Rev.* **1984**, 84, 577. (d) Huang, Y.-S.; Chaudret, B.; Bellan, J.; Mazières, M.-R. *Polyhedron* **1991**, 10, 2229.
9. Redmore, D. *J. Org. Chem.* **1970**, 35, 4114.
10. Kraus, W.; Weisert, A. Offenlegungsschrift 2738194, Germany, 1987.
11. Edmundson, R.S. in *The Chemistry of Organophosphorus Compounds*, Vol. 4, Hartley, F.R., Ed., Wiley: Chichester, England 1996, Chapter 2.
12. Loran, J.S.; Naylor, R.A.; Williams, A. *J. Chem. Soc., Perkin Trans. II* **1976**, 1444.
13. (a) Ten Hoeve, W.; Wynberg, H. *J. Org. Chem.* **1985**, 50, 4508. (b) Van der Haest, A.D. PhD thesis, University of Groningen, 1992.
14. (a) Hu, X., Ph.D thesis, University of Groningen 1995, (b) Hu, X; Kellogg, R.M. *Synthesis* **1995**, 533.
15. (a) Ebens, R.H.E., Ph.D thesis, University of Groningen, 1993. (b) Ebens, R.H.E.; Kellogg, R.M. *Recl. Trav. Chim. Pays-Bas* **1992**, 111, 56. (c) Sjouken, R.; Ebens, R.H.E.; Kellogg, R.M. *Recl. Trav. Chim. Pays-Bas* **1990**, 109, 552.
16. Hulst, R.; Zijlstra, R.W.J.; De Vries, N.K.; Feringa, B.L. *Tetrahedron: Asymmetry* **1994**, 5, 1701.
17. Munoz, A.; Hubert, C.; Luche, J.-L. *J. Org. Chem.* **1996**, 61, 6015.
18. Nagar, P.N. *Phosphorus, Sulfur and Silicon* **1993**, 79, 207.
19. Lesiak, K.; Uznanski, B.; Stec, W.J. *Phosphorus*, **1975**, 6, 65.

20. Jones, R.A.Y., *Physical and Mechanistic Organic Chemistry*, 2nd ed, Cambridge University Press: Cambridge, 1987, pp. 20-21.
21. Maryanoff, B.E.; Hutchins, R.O.; Maryanoff, C.A. in *Topics in Stereochemistry* Vol. 11, Allinger, N.L.; Eliel, E., Eds.; Wiley: New York, 1979, p. 187.
22. Bentrude, W.G. in *Phosphorus-31 NMR Spectral Properties in Compound Characterization and Structural Analysis*, Quin, L.D.; Verkade, J.G., Eds; VCH: New York, 1994, p. 41.
23. (a) Killean, R.C.G.; Lawrence, J.L.; Magennis, I.M. *Acta Cryst.* **1971**, B27, 189. (b) Craig, D.C.; Toia, R.F.; Wachter, V.J. *Aust. J. Chem.* **1989**, 42, 977.
24. Thiel, W.R.; Priermeier, T.; Bog, T. *J. Chem. Soc., Chem. Commun.* **1995**, 1871.
25. Maryanoff, B.E.; Hutchins, R.O.; Maryanoff, C.A. in *Topics in Stereochemistry*, Vol 11, Allinger, N.L.; Eliel, E., Eds.; Wiley: New York, 1979, p. 187.
26. Corbridge, D.E.C. *Phosphorus. An Outline of its Chemistry, Biochemistry and Technology*, Elsevier Science Publishers, Amsterdam, The Netherlands, 1990. See also: Hartley, F.R. in *The Chemistry of Organophosphorus Compounds*, Vol 1. Hartley, F.R., Ed. Wiley: Chichester, England 1990, p. 1.
27. Bentrude, W.G. in *Phosphorus-31 NMR Spectral Properties in Compound Characterization and Structural Analysis*, Quin, L.D.; Verkade, J.G., Eds.; VCH: New York, 1994, p. 41.
28. Anteunis, M.; Tavernier, D.; Borremans, F. *Bull. Chim. Soc. Belges* **1996**, 75, 396.
29. Corbridge, D.E.C. *The Structure Chemistry of Phosphorus*, Elsevier: Amsterdam, 1974.
30. (a) Bentrude, W.G.; Yee, K.C. *J. Chem. Soc., Chem. Commun.* **1972**, 169. (b) Bentrude, W.G.; Tan, H.-W. *J. Am. Chem. Soc.* **1973**, 95, 4666. (c) Bentrude, W.G.; Tan, H.-W.; Yee, K.C. *J. Am. Chem. Soc.* **1975**, 97, 573.
31. Van Nuffel, P.; Van Alsenoy, C.; Lenstra, A.T.H.; Geise, H.J. *J. Mol. Struct.* **1984**, 125, 1.
32. *Gaussian 94, Revision B.3*, Frisch, M.J.; Trucks, G.W.; Schlegel, H.B.; Gill, P.M.W.; Johnson, B.G.; Robb, M.A.; Cheeseman, J.R.; Keith, T.; Petersson, G.A.; Montgomery, J.A.; Raghavachari, K.; Allaham, M.A.; Zakrzewski, V.G.; Ortiz, J.V.; Foresman, J.B.; Peng, C.Y.; Ayala, P.Y.; Chen, W.; Wong, M.W.; Andres, J.L.; Replogle, E.S.; Gomperts, R.; Martin, R.L.; Fox, D.J.; Binkley, J.S.; Defrees, D.J.; Baker, J.; Stewart, J.P.; Head-Gordon, M.; Gonzales, C.; Pople, J.A. Gaussian, Inc., Pittsburgh PA, 1995.
33. (a) Pietro, W.S.; Francl, M.M.; Hehre, W.J.; Defrees, D.J.; Pople, J.A.; Binkley, J.S. *J. Am. Chem. Soc.* **1982**, 104, 5039. (b) Francl, M.M.; Pietro, W.S.; Hehre, W.J.; Binkley, J.S.; Gordon, M.S.; Defrees, D.J.; Pople, J.A. *J. Chem. Phys.* **1982**, 77, 3654. (c) Frisch, M.J.; Pople, J.A.; Binkley, J.S. *J. Chem. Phys.* **1984**, 80, 3265.